On the Mechanism of Laminar Damping of Oscillatory Waves Due to Bottom Friction

AUTHOR(S):

IWAGAKI, Yuichi; TSUCHIYA, Yoshito; CHEN, Huoxiong

CITATION:

IWAGAKI, Yuichi ...[et al]. On the Mechanism of Laminar Damping of Oscillatory Waves Due to Bottom Friction. Bulletin of the Disaster Prevention Research Institute 1967, 16(3): 49-75

ISSUE DATE:

1967-02-28

URL:

http://hdl.handle.net/2433/124723

Bull. Disas. Prev. Res. Inst. Kyoto Univ., Vol. 16, Part 3, No. 116, March, 1967

On the Mechanism of Laminar Damping of Oscillatory Waves Due to Bottom Friction

By Yuichi IWAGAKI, Yoshito TSUCHIYA and Huoxiong CHEN

(Manuscript received December 10, 1966)

Abstract

The purpose of this paper is to discover the mechanism of the laminar damping of oscillatory waves due to bottom friction with the aid of both the theory of the laminar boundary layer caused by waves and the measurements of the shearing stress and wave amplitude attenuation. In a theoretical approach the effects of convective terms involved in the basic equations of laminar boundary layers developing both on the bottom and the side walls of a wave channel, are considered on the basis of an approximate solution of the equation, and a theory of the laminar damping of Airy waves is established. In experimental studies, furthermore, direct measurements of instantaneous shearing stresses and observations of wave amplitude attenuation were performed, and the experimental results are compared with both the above theory and the linearized one.

1. Introduction

The phenomenon of wave damping due to bottom friction is not only of interest as a problem in fluid mechanics, but of practical significance in forecasting ocean waves and determining the design wave for coastal structures in shallow water.

The present paper is part of the results obtained from basic studies on the wave damping due to bottom friction which have been carried out for several years at the Ujigawa Hydraulic Laboratory, Disaster Prevention Research Institute.

Up to the present, the wave damping due to internal friction caused by viscosity has been investigated theoretically by Lamb[1] for deep water waves and Hough[2] and Biesel[3] for shallow water waves on the basis of the small amplitude wave theory.

It is concluded from their studies, however, that the wave damping due to internal friction has generally little effect on the coastal waves treated in this paper. With respect to the wave damping due to bottom friction, on the other hand, in 1949 Putnam and Johnson[4] made practical studies, but it seems that they fail to provide an adequate description of the characteristics of flow near the sea bottom, that is the boundary layer developing in association with oscillatory wave motion. In 1953, some experiments on the wave damping due to bottom friction and percolation over a permeable bed were made by Savage[5], and the experimental results were compared with the theory by Putnam and Johnson. He also investigated the relationship between the formation of sand waves and the wave energy

dissipation. In addition to bottom friction, there is the phenomenon of percolation in the energy dissipation on a sea bottom as discussed in Savage's paper. On this subject, Putnam[6] made a theoretical investigation, and later the same problem was re-examined by Reid and Kajiura[7], using a more rigorous approach than that employed by Putnam. As a result, a misinterpretation was discovered in Putnam's paper. Recently such problems were investigated theoretically by Hunt[8] and Murray[9], taking a viscous flow on the permeable boundary surface into account, and the result of the theory developed by Hunt agreed well with Savage's measurements for both permeable and impermeable smooth beds. On the other hand, in Japan an investigation on wave damping was made by Kishi[10] using the same procedure as that used by Putnam and the friction factor off the Niigata coast was estimated. The authors observed wave damping off actual coasts and also estimated friction factors of these coasts[11,12].

In studying the phenomenon of wave damping due to bottom friction, it is necessary to analyze the behavior of the boundary layer developing on a sea bottom. Regarding the development of the boundary layer, Eagleson[13,14], Grosch and Lukasik[15,16], and the authors[17,18,19,20] have carried out experimental studies on the wave damping due to bottom friction and the results were compared with the formula of wave damping derived on the basis of the linearized, laminar boundary layer theory. It was found from the comparison that there are wide differences between the theoretical and experimental values. Kajiura[21] developed a theory of the turbulent boundary layer on a smooth bed due to oscillatory currents and proposed a relationship between the friction factor and the Reynolds number. Jonsson[22,23] also attempted to estimate the relationship of the friction factor against the Reynolds number for both laminar and turbulent boundary layer on the basis of his velocity measurements in the turbulent boundary layer on a rough bed[24].

Most recently Van Dorn[25] carried out precise experiments of laminar wave damping for dispersive oscillatory waves and compared the results of his theory, taking account of the energy dissipation on the water surface. Although, the results of these experiments agree well with the theoretical ones, it seems that the formula of the surface damping coefficient derived by assuming the free surface to be horizontally immobilized is questionable.

The purpose of the present studies is to discover the mechanism of the laminar damping of oscillatory waves. For this an approximate solution of the non-linear laminar boundary layer equations is derived by means of the perturbation method, and the effects of the convective terms in the equations on the bottom shearing stress and wave energy dissipation are clarified. The theoretical results for bottom shearing stresses are compared with the results of the direct measurement of them. With regard to the wave damping, a theory of laminar damping due to both bottom and side wall frictions is presented on the basis of the above laminar boundary layer theory, and the theoretical result is compared with the results of the experiment of wave amplitude attenuation and the linearized theory.

2. Theory of wave damping due to bottom friction

(1) Laminar boundary layer theory

With regard to the boundary layer growth resulting from wave motion, for a solitary wave Iwasa[26] made an analytical investigation applying the momentum integral equation of the boundary layer and obtained interesting results on the laminar boundary layer growth and the wave damping. There is only a linearized theory of the laminar boundary layer, based on Stokes' solution, of which the validity has been examined by comparing it with the experimental results obtained by Eagleson,[13,14] Grosch and Lukasik[15,16], and the authors[17,18]. However, it has not yet been made clear how the convective terms involved in the basic equation of the laminar boundary layer influence the boundary layer growth. Grosch[27] has already derived a solution of the non-linear boundary layer equation in the form of a power series by using Glauert's method, but it seems that the solution is inadequate because it is impossible to examine the phenomenon over a whole period. Therefore, the authors derive an approximate solution of the laminar boundary layer equation written in dimensionless forms by means of Lighthill's method. With regard to the boundary layer developing both on the bottom and the side walls of a wave channel, the effects of the convective terms on the shearing stress are investigated on the basis of the above solution.

(a) *Laminar boundary layer developing on the bottom of a wave channel*

Taking the axis of x in the direction of the wave propagation and the axis of z perpendicular to the bottom and denoting the velocity components in these directions by u and w respectively, the two-dimensional laminar boundary layer equations for the unsteady, incompressible fluid are written as:

$$\left.\begin{aligned} &\frac{\partial u}{\partial t}+u\frac{\partial u}{\partial x}+w\frac{\partial u}{\partial z}=-\frac{1}{\rho}\frac{\partial p}{\partial x}+\nu\frac{\partial^2 u}{\partial z^2}, \\ &\frac{\partial u}{\partial x}+\frac{\partial w}{\partial z}=0, \quad -\frac{1}{\rho}\frac{\partial p}{\partial x}=\frac{\partial U}{\partial t}+U\frac{\partial U}{\partial x}, \end{aligned}\right\} \qquad \cdots\cdots(1)$$

in which t is the time, p the pressure, ν the kinematic viscosity of water, ρ the density and U the velocity just outside the boundary layer, to which the relation derived from the wave theory is applied. Now, introducing a representative velocity u_0, the wave length L and the wave celerity c, and using the dimensionless quantities defined as follows:

$$\left.\begin{aligned} &u=\bar{u}u_0,\ w=\frac{u_0\bar{w}}{\sqrt{R}},\ U=u_0\bar{U}, \\ &p=\rho u_0^2\bar{p},\ R=\frac{cL}{2\pi\nu},\ x=\left(\frac{L}{2\pi}\right)\xi, \\ &z=\left(\frac{L}{2\pi\sqrt{R}}\right)\zeta,\ t=\left(\frac{L}{2\pi c}\right)\tau, \end{aligned}\right| \qquad \cdots\cdots(2)$$

Eq. (1) can be written as:

$$\left.\begin{aligned}&\frac{\partial\bar{u}}{\partial\tau}+\left(\frac{u_0}{c}\right)\left\{\bar{u}\frac{\partial\bar{u}}{\partial\xi}+\bar{w}\frac{\partial\bar{u}}{\partial\zeta}\right\}=-\frac{\partial\bar{p}}{\partial\xi}+\frac{\partial^2\bar{u}}{\partial\zeta^2},\\&\frac{\partial\bar{u}}{\partial\xi}+\frac{\partial\bar{w}}{\partial\zeta}=0,\quad -\frac{\partial\bar{p}}{\partial\xi}=\frac{\partial\bar{U}}{\partial\tau}+\left(\frac{\bar{u}_0}{c}\right)\bar{U}\frac{\partial\bar{U}}{\partial\xi}\end{aligned}\right\}\quad\cdots\cdots(3)$$

with the initial conditions that $\bar{u}=0$ at $\tau=0$, $u=0$ at $\zeta=0$ and $\bar{u}=\bar{U}$ at $\zeta\to\infty$.

Taking account of progressive waves on the basis of Airy's wave theory and applying the maximum velocity component at a bottom $u_{b\,\max}$ to u_0, the following relationships are obtained:

$$\left.\begin{aligned}&\bar{U}=\sin(\xi-\tau),\quad -\frac{\partial\bar{p}}{\partial\xi}=-\cos(\xi-\tau)+\left(\frac{1}{2}\right)\left(\frac{u_0}{c}\right)\sin 2(\xi-\tau),\\&u_0=u_{b\,\max}=\frac{\pi H}{T\sinh kh},\quad k=\frac{2\pi}{L},\\&\frac{u_0}{c}=\frac{u_{b\,\max}}{c}=\frac{\pi H}{L\sinh kh}\ll 1.\end{aligned}\right\}\quad\cdots\cdots(4)$$

Expressing the solutions of $\bar{u}$ and $\bar{w}$ respectively by

$$\left.\begin{aligned}&\bar{u}=\bar{u}_0+\varepsilon\bar{u}_1+\varepsilon^2\bar{u}_2+\cdots\cdots,\\&\bar{w}=\bar{w}_0+\varepsilon\bar{w}_1+\varepsilon^2\bar{w}_2+\cdots\cdots,\end{aligned}\right\}\quad\cdots\cdots(5)$$

the solution of Eq. (3) can be obtained by the perturbation method with a parameter of ε which is equal to u_0/c. Substituting these expressions into Eq. (3) and satisfying the relation between each coefficient of the terms on both sides, multiplied by the ascending powers of ε, a family of equations is obtained as follows: For $\bar{u}_0$ and $\bar{w}_0$,

$$\left.\begin{aligned}&\frac{\partial\bar{u}_0}{\partial\tau}-\frac{\partial^2\bar{u}_0}{\partial\zeta^2}=-\cos(\xi-\tau),\\&\frac{\partial\bar{u}_0}{\partial\xi}+\frac{\partial\bar{w}_0}{\partial\zeta}=0,\end{aligned}\right\}\quad\cdots\cdots(6)$$

which is identical with that for one-dimensional heat conduction. The initial and boundary conditions for Eq. (6) are: $\bar{u}_0=0$ at $\tau=0$ and $\zeta=0$, and $\bar{u}_0=\bar{U}=\sin(\zeta-\tau)$ at $\zeta\to\infty$. Eq. (6) is for the so-called linearized theory and its solution has been derived by Grosch[27] in the form

$$\left.\begin{aligned}\bar{u}_0=&\sin(\xi-\tau)-e^{-\frac{\zeta}{\sqrt{2}}}\sin\left(\xi-\tau+\frac{1}{\sqrt{2}}\zeta\right)\\&+\frac{2}{\pi}\int_0^\infty e^{(\xi-\tau)\sigma^2}\frac{\sigma\sin(\zeta\sigma)}{1+\sigma^4}d\sigma.\end{aligned}\right\}\quad\cdots\cdots(7)$$

In the above equation, the third term on the right vanishes when τ becomes sufficiently large. Therefore, taking only the so-called steady state solution into account, the third term can be omitted.

Next, the equations for $\bar{u}_1$ and $\bar{w}_1$ can be written together with the initial and boundary conditions as follows:

$$\left.\begin{aligned}&\frac{\partial \bar{u}_1}{\partial \tau}-\frac{\partial^2 \bar{u}_1}{\partial \zeta^2}=-\left(\bar{u}_0\frac{\partial \bar{u}_0}{\partial \xi}+\bar{w}_0\frac{\partial \bar{u}_0}{\partial \zeta}\right)+\bar{U}\frac{\partial \bar{U}}{\partial \xi},\\&\frac{\partial \bar{u}_1}{\partial \xi}+\frac{\partial \bar{w}_1}{\partial \zeta}=0,\ \bar{u}_1=\bar{w}_1=0\,;\ \tau=\zeta=0,\ \zeta\to\infty.\end{aligned}\right\}\quad\cdots\cdots(8)$$

In general, the expression for $\bar{u}_t$ can formally be written in the form

$$\left.\begin{aligned}&\frac{\partial \bar{u}_t}{\partial \tau}-\frac{\partial^2 \bar{u}_t}{\partial \zeta^2}=F_t(\xi,\ \tau,\ \zeta),\ \ \frac{\partial \bar{u}_t}{\partial \xi}+\frac{\partial \bar{w}_t}{\partial \zeta}=0,\\&\bar{u}_t=\bar{w}_t=0\,;\ \tau=\zeta=0,\ \zeta\to\infty\end{aligned}\right\}\quad\cdots\cdots(9)$$

together with the initial and boundary conditions.

Since this is a heat conduction type equation, the solution for $\bar{u}_t$ can be found by applying Green's function $H(\zeta,\ \tau\,;\ q,\ s)$ and the solution for $\bar{u}$ by the perturbation method can formally be expressed as:

$$\begin{aligned}\bar{u}(\xi,\ \tau,\ \zeta)=\bar{u}_0&+\varepsilon\int_0^\tau ds\int_0^\infty H(\zeta,\ \tau:q,\ s)F_1(q,\ s)dq\\&+\varepsilon^2\int_0^\tau ds\int_0^\infty H(\zeta,\ \tau:q,\ s)F_2(q,\ s)dq\\&+\cdots\cdots,\end{aligned}\qquad\cdots\cdots(10)$$

in which

$$\begin{aligned}H(\zeta,\ \tau:q,\ s)=&\left\{\frac{1}{2\sqrt{\pi(\tau-s)}}\right\}\\&\times\left[\exp\left\{-\frac{(\zeta-q)^2}{4(\tau-s)}\right\}-\exp\left\{-\frac{(\zeta+q)^2}{4(\tau-s)}\right\}\right];\ \tau>s,\\=&0\,;\ \tau<s.\end{aligned}\qquad\cdots\cdots(11)$$

Since the integration of the above equation is complicated, taking into consideration the form of function $F_t(q,\ s)$, only the steady state solution is considered in the subsequent descriptions. The steady state solutions for $\bar{u}_0$ and $\bar{w}_0$ can be written in the form

$$\left.\begin{aligned}&\bar{u}_0=\sin(\xi-\tau)-e^{-\frac{\zeta}{\sqrt{2}}}\sin\left(\xi-\tau+\frac{1}{\sqrt{2}}\zeta\right),\\&-\bar{w}_0=\zeta\cos(\xi-\tau)-e^{-\frac{\zeta}{\sqrt{2}}}\sin\left(\xi-\tau+\frac{1}{\sqrt{2}}\zeta-\frac{\pi}{4}\right)\\&\qquad+\sin\left(\xi-\tau-\frac{\pi}{4}\right).\end{aligned}\right\}\quad\cdots\cdots(12)$$

Substituting these relationships for $\bar{u}_0$ and $\bar{w}_0$ into Eq. (8), the equation for $\bar{u}_1$ becomes finally

$$\begin{aligned}\frac{\partial \bar{u}_1}{\partial \tau}-\frac{\partial^2 \bar{u}_1}{\partial \zeta^2}=\frac{1}{2}&\left\{e^{-\frac{\zeta}{\sqrt{2}}}\cos\left(\frac{1}{\sqrt{2}}\zeta\right)\right.\\&\left.+\zeta e^{-\frac{\zeta}{\sqrt{2}}}\cos\left(\frac{1}{\sqrt{2}}\zeta-\frac{\pi}{4}\right)\right\}\sin 2(\xi-\tau)\end{aligned}$$

$$+\frac{1}{2}\left\{e^{-\frac{\zeta}{\sqrt{2}}}\sin\left(\frac{1}{\sqrt{2}}\zeta\right)\right.$$
$$\left.-\zeta e^{-\frac{\zeta}{\sqrt{2}}}\sin\left(\frac{1}{\sqrt{2}}\zeta-\frac{\pi}{4}\right)\right\}\cos 2(\xi-\tau)$$
$$+\frac{1}{2}\left\{\zeta e^{-\frac{\zeta}{\sqrt{2}}}\sin\left(\frac{1}{\sqrt{2}}\zeta-\frac{\pi}{4}\right)\right.$$
$$\left.+e^{-\frac{\zeta}{\sqrt{2}}}\cos\left(\frac{1}{\sqrt{2}}\zeta\right)-e^{-\frac{\zeta}{\sqrt{2}}}\right\}. \quad \cdots\cdots(13)$$

Following Schlichting's procedure[28], the solution of Eq. (13) which satisfies the boundary conditions that $\bar{u}_1=0$ at $\zeta=0$ and $\partial\bar{u}_1/\partial\zeta=0$ at $\zeta\to\infty$, can easily be derived, and an approximate solution for $\bar{u}$ can finally be written in the form

$$\bar{u}=\sin(\xi-\tau)-e^{-\frac{\zeta}{\sqrt{2}}}\sin\left(\xi-\tau+\frac{1}{\sqrt{2}}\zeta\right)$$
$$+\varepsilon\left[\left\{\frac{11}{18}e^{-\zeta}\sin\zeta-\frac{7}{18}e^{-\frac{\zeta}{\sqrt{2}}}\sin\left(\frac{1}{\sqrt{2}}\zeta\right)\right.\right.$$
$$\left.+\frac{1}{6}\zeta e^{-\frac{\zeta}{\sqrt{2}}}\sin\left(\frac{1}{\sqrt{2}}\zeta-\frac{\pi}{4}\right)\right\}\sin 2(\xi-\tau)$$
$$+\left\{-\frac{11}{18}e^{-\zeta}\cos\zeta+\frac{11}{18}e^{-\frac{\zeta}{\sqrt{2}}}\cos\left(\frac{1}{\sqrt{2}}\zeta\right)\right.$$
$$\left.+\frac{1}{6}\zeta e^{-\frac{\zeta}{\sqrt{2}}}\cos\left(\frac{1}{\sqrt{2}}\zeta-\frac{\pi}{4}\right)\right\}\cos 2(\xi-\tau)$$
$$+\left\{\frac{1}{4}e^{-\frac{\zeta}{\sqrt{2}}}+\frac{1}{2}e^{-\frac{\zeta}{\sqrt{2}}}\sin\left(\frac{1}{\sqrt{2}}\zeta\right)-e^{-\frac{\zeta}{\sqrt{2}}}\cos\left(\frac{1}{\sqrt{2}}\zeta\right)\right.$$
$$\left.\left.-\frac{1}{2}\zeta e^{-\frac{\zeta}{\sqrt{2}}}\sin\left(\frac{1}{\sqrt{2}}\zeta+\frac{\pi}{4}\right)+\frac{3}{4}\right\}\right]+0(\varepsilon^2). \quad \cdots\cdots(14)$$

From this result, it is found that only the constant term on the right of Eq. (14) remains, taking the average of $\bar{u}$ with respect to time at $\zeta\to\infty$, just outside the boundary layer, and that there exists a certain mass transport velocity which can be expressed by

$$\bar{u}_m=\frac{3}{4}\varepsilon \quad \cdots\cdots(15)$$

This can be rewritten in the form

$$u_m=\left(\frac{3}{16}\right)\left(\frac{2\pi}{T}\right)\frac{H^2k}{\sinh^2 kh} \quad \cdots\cdots(16)$$

which is identical with that obtained by Lonquet-Higgins[29].

Applying the above result, a theoretical formula for the bottom shearing stress can be derived. The shearing stress on the bottom is generally given by the relationship $\tau_0=\mu(\partial u/\partial z)_{z=0}$ for laminar flows. Expressing this in the dimensionless form and using Eq. (5), the shearing stress can be written as

$$\frac{\tau_0}{\rho u_0^2}=R_e^{-\frac{1}{2}}\left\{\sin\left(\xi-\tau-\frac{\pi}{4}\right)+\varepsilon\left(\frac{\partial\bar{u}_1}{\partial\zeta}\right)_{\zeta=0}\right.$$

$$+\varepsilon^2\left(\frac{\partial \bar{u}_2}{\partial \zeta}\right)_{\zeta=0}+\cdots\cdots\cdots\Big\}. \quad \cdots\cdots(17)$$

Calculating the above equation with the relationship of Eq. (14), the following equation is obtained as an approximate solution for τ_0:

$$\frac{\tau_0}{\rho u_0^2} \approx R_e^{-\frac{1}{2}}\Big[\sin\Big(\xi-\tau-\frac{\pi}{4}\Big)+\varepsilon\Big(\frac{1}{2\sqrt{2}}+\Big(\frac{11}{18}-\frac{5\sqrt{2}}{18}\Big)\sin 2(\xi-\tau)$$
$$+\Big(\frac{11}{18}-\frac{4\sqrt{2}}{18}\Big)\cos 2(\xi-\tau)\Big\}+0(\varepsilon^2)\Big], \quad \cdots\cdots(18)$$

in which

$$R_e=\frac{\pi}{2\sinh^2 kh}\Big(\frac{cH}{\nu}\Big)\Big(\frac{H}{L}\Big)=\frac{1}{2\pi}\frac{u_0^2 T}{\nu}. \quad \cdots\cdots(19)$$

The first term in the brackets of Eq. (18) indicates the results based on the linearized theory and the second term indicates the effect of the convective terms. In Fig. 1, the calculated results of Eq. (18) are shown by using the value of $\varepsilon=\pi(H/L)/\sinh kh$ as a parameter and also the time variation of the dimensionless water surface profile $\bar{\eta}$ for the purpose of comparison. It is found from the figure that the characteristics of the shearing stress vary slightly with the value of ε, but the effect of ε may be negligible because the value will not exceed about 0.15 for the waves treated in practice.

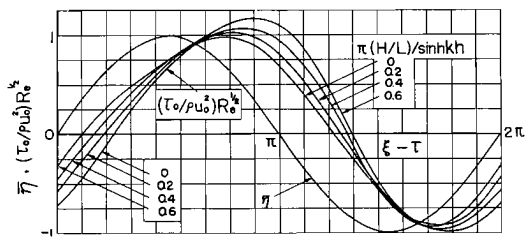

Fig. 1. Effect of convective terms in boundary layer equation on bottom shearing stress.

According to Eagleson's study, the average bottom friction coefficient is defined by

$$\overline{C}_f=\frac{2\bar{\tau}_0}{\rho\overline{U}^2} \quad \cdots\cdots(20)$$

in which $\bar{\tau}_0$ and $\overline{U}^2$ are the average values of τ_0 and U^2 expressed by Eqs. (18) and (4) respectively. Since it is complicated to calculate $\overline{C}_f$ directly by Eq. (17), the results obtained by the graphical integration are shown in Fig. 2. Each of the curves (a), (b) and (c), indicates how the phase interval is to be chosen in taking the time average ; (a) resulted when the absolute value of τ_0 was averaged with respect to time from the phase θ when $\tau_0=0$ to $\theta+2\pi$, and (b) and (c) resulted when τ_0 was averaged over the phase intervals corresponding to the

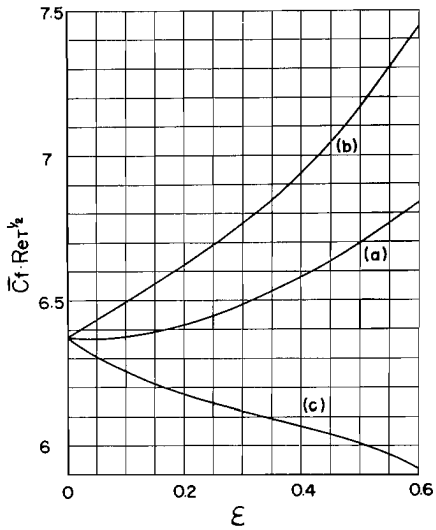

Fig. 2. Effect of convective terms in boundary layer equation on bottom friction coefficient $\overline{C}_f$.

positive and negative values of τ_0 respectively. In the figure, the wave Reynolds number R_{eT} is expressed as

$$R_{eT}=2\pi R_e=\left(\frac{u_0 H}{\nu}\right)\left(\frac{u_0 T}{H}\right)=\frac{u_0^2 T}{\nu}. \quad \cdots\cdots(21)$$

In the case of the linearized theory where the value of ε vanishes, the friction coefficient $\overline{C}_f$ is expressed as

$$\overline{C}_f=8\sqrt{\frac{2}{\pi}}R_{eT}^{-\frac{1}{2}} \quad \cdots\cdots(22)$$

(b) *Laminar boundary layer developing on the side walls of a wave channel*

In the experiment on wave damping, the energy dissipation due to the friction acting on the side walls of a wave channel must be considered when the width of a wave channel is small compared with the water depth, so that it is necessary to clarify the behavior of boundary layers developing on the side walls.

Taking the axis of z vertically along the side walls and the axis of y perpendicular to it, and using the same notations as those in Eq. (1), the boundary layer equations for this case are expressed as

$$\left.\begin{aligned}
&\frac{\partial u}{\partial t}+u\frac{\partial u}{\partial x}+v\frac{\partial u}{\partial y}+w\frac{\partial u}{\partial z}=-\frac{1}{\rho}\frac{\partial p}{\partial x}+\nu\frac{\partial^2 u}{\partial y^2},\\
&\frac{\partial w}{\partial t}+u\frac{\partial w}{\partial x}+v\frac{\partial w}{\partial y}+w\frac{\partial w}{\partial z}=g-\frac{1}{\rho}\frac{\partial p}{\partial z}+\nu\frac{\partial^2 w}{\partial y^2},\\
&\frac{\partial u}{\partial x}+\frac{\partial v}{\partial y}+\frac{\partial w}{\partial z}=0,
\end{aligned}\right\} \quad \cdots\cdots(23)$$

in which g is the acceleration of gravity and v the velocity component in the

direction of y. Using the dimensionless quantities, $v=u_0\bar{v}/\sqrt{R}$, $P=\rho u_0^2\bar{p}-(\rho gL/2\pi)\zeta$, and $y=(L/2\pi)\eta/\sqrt{R}$ in addition to Eq. (2), the above equation can be written as

$$\left.\begin{aligned}
&\frac{\partial u}{\partial\tau}+\varepsilon\left(\bar{u}\frac{\partial u}{\partial\xi}+\bar{v}\frac{\partial\bar{u}}{\partial\eta}+\overline{w}\frac{\partial\bar{u}}{\partial\zeta}\right)=-\frac{\partial\bar{p}}{\partial\xi}+\frac{\partial^2\bar{u}}{\partial\eta^2},\\
&\frac{\partial\overline{w}}{\partial\tau}+\varepsilon\left(\bar{u}\frac{\partial\overline{w}}{\partial\xi}+\bar{v}\frac{\partial\overline{w}}{\partial\eta}+\overline{w}\frac{\partial\overline{w}}{\partial\zeta}\right)=-\frac{\partial\bar{p}}{\partial\zeta}+\frac{\partial^2\overline{w}}{\partial\eta^2},\\
&\frac{\partial\bar{u}}{\partial\xi}+\frac{\partial\bar{v}}{\partial\eta}+\frac{\partial\overline{w}}{\partial\zeta}=0.
\end{aligned}\right\}\quad\cdots\cdots\cdots\cdots(24)$$

To derive the solution of Eq. (24) by the perturbation method, using the forms

$$\left.\begin{aligned}
&\bar{u}=\bar{u}_0+\varepsilon\bar{u}_1+\varepsilon^2\bar{u}_2+\cdots\cdots,\\
&\bar{v}=\bar{v}_0+\varepsilon\bar{v}_1+\varepsilon^2\bar{v}_2+\cdots\cdots,\\
&\overline{w}=\overline{w}_0+\varepsilon\overline{w}_1+\varepsilon^2\overline{w}_2+\cdots\cdots,
\end{aligned}\right\}\quad\cdots\cdots\cdots\cdots(25)$$

a family of the equations corresponding to Eqs. (6) and (8) together with the boundary conditions can be written as follows:

For u_0 and w_0,

$$\left.\begin{aligned}
&\frac{\partial\bar{u}_0}{\partial\tau}-\frac{\partial^2\bar{u}_0}{\partial\eta^2}=\frac{\partial\bar{U}}{\partial\tau},\quad \frac{\partial\overline{w}_0}{\partial\tau}-\frac{\partial^2\overline{w}_0}{\partial\eta^2}=\frac{\partial\overline{W}}{\partial\tau},\\
&\frac{\partial\bar{u}_0}{\partial\xi}+\frac{\partial\bar{v}_0}{\partial\eta}+\frac{\partial\overline{w}_0}{\partial\zeta}=0,\\
&\bar{u}_0=w_0=0\,;\ \eta=0,\ \bar{u}_0=\bar{U}\ \text{and}\ \overline{w}_0=\overline{W}\,;\ \eta\to\infty,
\end{aligned}\right\}\quad\cdots\cdots\cdots\cdots(26)$$

and for $\bar{u}_1$ and $\overline{w}_1$,

$$\left.\begin{aligned}
&\frac{\partial\bar{u}_1}{\partial\tau}-\frac{\partial^2\bar{u}_1}{\partial\eta^2}=\bar{U}\frac{\partial\bar{U}}{\partial\xi}+\overline{W}\frac{\partial\bar{U}}{\partial\zeta}-\left(\bar{u}_0\frac{\partial\bar{u}_0}{\partial\xi}+\bar{v}_0\frac{\partial\bar{u}_0}{\partial\eta}+\overline{w}_0\frac{\partial\bar{u}_0}{\partial\zeta}\right),\\
&\frac{\partial\overline{w}_1}{\partial\tau}-\frac{\partial^2\overline{w}_1}{\partial\eta^2}=\bar{U}\frac{\partial\overline{W}}{\partial\xi}+\overline{W}\frac{\partial\overline{W}}{\partial\zeta}-\left(\bar{u}_0\frac{\partial\overline{w}_0}{\partial\xi}+\bar{v}_0\frac{\partial\overline{w}_0}{\partial\eta}+\overline{w}_0\frac{\partial\overline{w}_0}{\partial\zeta}\right),\\
&\frac{\partial\bar{u}_1}{\partial\xi}+\frac{\partial\bar{v}_1}{\partial\eta}+\frac{\partial\overline{w}_1}{\partial\zeta}=0,\\
&\bar{u}_1=\overline{w}_1=0\,;\quad\eta=0,\quad\frac{\partial\bar{u}_1}{\partial\eta}=\frac{\partial\overline{w}_1}{\partial\eta}=0\,;\quad\eta\to\infty,
\end{aligned}\right\}\quad\cdots\cdots\cdots\cdots(27)$$

in which $\bar{U}$ and $\overline{W}$ are the velocity components of water particles just outside the boundary layer on the side wall. Applying the relationships derived from Airy's wave theory in this case, the solutions for $\bar{u}$ and $\overline{w}$ calculated to the second approximation become finally

$$\begin{aligned}
\bar{u}=&\left\{\sin(\xi-\tau)-e^{-\frac{\eta}{\sqrt{2}}}\sin\left(\xi-\tau+\frac{1}{\sqrt{2}}\eta\right)\right\}\cosh\zeta\\
&+\varepsilon\Bigg[-\left\{e^{-\frac{\eta}{\sqrt{2}}}\sin\left(\frac{1}{\sqrt{2}}\eta\right)+\left(\frac{1}{4}\right)e^{-\sqrt{2}\eta}\sin(\sqrt{2}\eta)\right.\\
&\left.+e^{-\eta}\sin\eta\right\}\sin 2(\xi-\tau)+\left\{e^{-\frac{\eta}{\sqrt{2}}}\cos\left(\frac{1}{\sqrt{2}}\eta\right)\right.
\end{aligned}$$

$$+\left(-\frac{1}{4}\right)e^{-\sqrt{2}\eta}\cos(\sqrt{2}\eta)-\left(\frac{5}{4}\right)e^{-\eta}\cos\eta\Big\}\cos 2(\xi-\tau)\Big]+0(\varepsilon^2),$$

$$\bar{w}=-\left\{\cos(\xi-\tau)-e^{-\frac{\eta}{\sqrt{2}}}\cos\left(\xi-\tau+\frac{1}{\sqrt{2}}\eta\right)\right\}\sinh\zeta$$

$$+\varepsilon\left\{\frac{1}{4}e^{-\sqrt{2}\eta}+e^{-\frac{\eta}{\sqrt{2}}}\sin\left(\frac{1}{\sqrt{2}}\eta\right)-\frac{1}{4}\right\}\sinh 2\zeta+0(\varepsilon^2). \quad \cdots\cdots(28)$$

With regard to the mass transport, it can be seen from the above results that it does not exist in the direction of the wave propagation, but that in the vertical direction there exists a mass transport velocity expressed as

$$\bar{w}_m=-\frac{\varepsilon}{4}\sinh 2\zeta, \quad \cdots\cdots(29)$$

which is rewritten as

$$\bar{w}_m=-\left(\frac{1}{16}\right)\left(\frac{2\pi}{T}\right)\frac{H^2k}{\sinh^2 k}\sinh 2\zeta. \quad \cdots\cdots(30)$$

In the above equation, $\bar{w}_m$ vanishes at $\zeta=0$ and becomes maximum at the water surface.

Consider the shearing stresses acting on the side walls of a wave channel. Using Eq. (28), the relationships for these are derived as follows:

$$\frac{\tau_{0x}}{\rho u_0^2}=R_e^{-\frac{1}{2}}\Big[\sin\left(\xi-\tau-\frac{\pi}{4}\right)\cosh\zeta$$

$$+\varepsilon\left\{\left(1-\frac{3\sqrt{2}}{4}\right)\sin 2(\xi-\tau)\right.$$

$$\left.+\left(\frac{5}{4}-\frac{3\sqrt{2}}{4}\right)\cos 2(\xi-\tau)\right\}+0(\varepsilon^2)\Big] \quad \cdots\cdots(31)$$

in the x-direction and

$$-\frac{\tau_{0z}}{\rho u_0^2}=R_e^{-\frac{1}{2}}\Big[\cos\left(\xi-\tau-\frac{\pi}{4}\right)\sinh\zeta$$

$$-\varepsilon\frac{\sqrt{2}}{4}\sinh 2\zeta+0(\varepsilon^2)\Big] \quad \cdots\cdots(32)$$

in the z-direction, in which R_e is expressed by Eq. (19).

The above method of analysis in applying Airy's wave theory is also applicable in the case of waves accompanying the mass transport on a substantial scale, Stokes' waves for example, and the authors have already made some calculations regarding it which will be published at a later date.

(2) **Theory on wave damping**

In the subsequent descriptions, the wave damping due to friction is considered after the wave energy dissipation due to viscosity within the boundary layers on the bottom and side walls has been estimated on the basis of the non-linear laminar

boundary layer theory.

(a) *Wave energy dissipation within boundary layers* It is assumed that the wave energy is dissipated only by bottom friction due to viscosity. The rate of energy dissipation in an incompressive fluid due to viscosity per second per unit volume is written in terms of velocity gradients through Rayleigh's laminar dissipation function as

$$\Phi=\mu\left[2\left(\frac{\partial u}{\partial x}\right)^2+2\left(\frac{\partial w}{\partial z}\right)^2+\left\{\left(\frac{\partial w}{\partial x}\right)+\left(\frac{\partial u}{\partial z}\right)\right\}^2\right], \quad \cdots\cdots(33)$$

in which Φ is the rate of energy dissipation, known as the dissipation function. Neglecting the terms including w and $\partial u/\partial x$, which are quite small compared with $\partial u/\partial z$, the average rate of energy dissipation per unit area in a boundary layer E_{fb} can be approximately expressed as

$$\begin{aligned}\bar{E}_{fb}&\approx\frac{\mu}{L}\int_0^L\int_0^\delta\left(\frac{\partial u}{\partial z}\right)^2dzdx\\&\approx\frac{\mu u_0^2}{L}\sqrt{R}\int_0^{2\pi}\int_0^{\delta_\zeta}\left(\frac{\partial\bar{u}}{\partial\zeta}\right)^2d\zeta d\xi, \quad \cdots\cdots(34)\end{aligned}$$

in which μ is the dynamic viscosity of water and δ_ζ the dimensionless expression $(2\pi\sqrt{R}\delta/L)$ of the boundary layer thickness δ.

Calculating Eq. (34) with the aid of Eq. (14) yields

$$\bar{E}_{fb}\approx\frac{\mu}{2}\beta\left(\frac{\pi H}{T}\right)^2\mathrm{cosech}^2\,kh\left\{1-\frac{8\sqrt{2}}{3\pi}\left(\frac{11}{18}-\frac{91\sqrt{2}}{288}\right)\varepsilon+0(\varepsilon^2)\right\}. \quad \cdots\cdots(35)$$

This shows, needless to say, the energy dissipation when the effect of the convective terms involved in the boundary layer equation is taken into account. In the equation, the first term on the right is identical with that derived from the linearized theory and the second term indicates the effect of the convective terms. From this result, it is found that the rate of the energy dissipation is about 2% less than that in the linearized theory when the value of ε is assumed to be 0.2.

Since the average rate of energy dissipation per unit area of the side wall of a water tank $\bar{E}_{fw}$ can be calculated by

$$\begin{aligned}2\bar{E}_{fw}&\approx\frac{2\mu}{Lh}\int_0^h\int_0^L\int_0^\delta\left\{\left(\frac{\partial u}{\partial y}\right)^2+\left(\frac{\partial w}{\partial y}\right)^2\right\}dydxdz\\&\approx\frac{\mu u_0^2\sqrt{R}}{\pi h}\int_0^{kh}\int_0^{2\pi}\int_0^{\delta\eta}\left\{\left(\frac{\partial\bar{u}}{\partial\eta}\right)^2+\left(\frac{\partial\bar{w}}{\partial\eta}\right)^2\right\}d\eta d\xi d\zeta, \quad \cdots\cdots(36)\end{aligned}$$

substituting Eq. (28) into this, the integration yields

$$2\bar{E}_{fw}\approx\frac{\mu}{kh}\beta\left(\frac{\pi H}{T}\right)^2\coth kh\left\{1+\frac{8\sqrt{2}}{3\pi}\left(\frac{11}{12}-\frac{\sqrt{2}}{120}\right)\varepsilon\,\mathrm{sech}\,kh+0(\varepsilon^2)\right\}. \quad \cdots(37)$$

From the above result, it is considered that the effect of the convective terms on the rate of energy dissipation on the side wall is of the order of $\varepsilon\,\mathrm{sech}\,kh$. However in the authors' experiment the maximum value becomes as much as 20% of that of the linearized theory.

Now, denoting the width of a water tank by B and the ratio of the energy dissipation in boundary layers on the bottom to that on the side walls by ψ, the following approximate relationship can be obtained:

$$\psi=\frac{\bar{E}_{fb}B}{2\bar{E}_{fw}h}\approx\frac{kB}{\sinh 2kh}\left\{1-(1.086\,\mathrm{sech}\,kh+0.197)\varepsilon\right\}. \quad \cdots\cdots(38)$$

In the above equation, the relation corresponding to the case when ε vanishes is identical with what is called Keulegan's method presented in Savage's paper which is derived from the linearized theory.

(b) *Mechanism of wave damping* The relationship of the wave energy conservation for a two-dimensional case, under the assumption that the energy is dissipated by bottom friction only, is given by

$$\frac{d(C_gE)}{dx}=-\bar{E}_{fb}, \quad \cdots\cdots(39)$$

in which C_g is the group velocity and E the wave energy per unit area.

Substituting the relationships for C_g and E derived from Airy's wave theory into Eq. (39), and integrating under the assumptions that $H=H_0$ at $x=0$ and ε is taken to be constant, yields

$$H=H_0\exp\left(\frac{-\epsilon_b x}{L}\right), \quad \cdots\cdots(40)$$

in which

$$\left.\begin{aligned}&\epsilon_b\approx\left(\frac{4\pi^2}{\beta L}\right)\frac{1-0.197\varepsilon}{\sinh 2kh+2kh},\\&\beta=\left(\frac{\pi}{\nu T}\right)^{\frac{1}{2}}.\end{aligned}\right\} \quad \cdots\cdots(41)$$

It is concluded from the above equation that the effect of the convective terms on ϵ_b becomes at most 3% for the waves made in the authors' experiment. In addition, the expression for ϵ_b in the case when $\varepsilon=0$ agrees with that obtained by Eagleson and is called the dimensionless decay modulus. On the other hand, another expression for the relationship of Eq. (40) was established by one of the authors[17].

Instead of Eq. (39), the following equation must be used when the energy dissipation due to side wall friction is taken into account in addition to that due to bottom friction:

$$\frac{d(C_gEB)}{dx}=-(\bar{E}_{fb}B+2\bar{E}_{fw}h)=-\bar{E}_{fb}B\left(1+\frac{1}{\psi}\right). \quad \cdots\cdots(42)$$

Thus, denoting the decay modulus based on both bottom and side wall frictions by ϵ_{b+w}, the relationship of wave damping corresponding to Eq. (40) becomes

$$\left.\begin{aligned}&H=H_0\exp\left(\frac{-\epsilon_{b+w}x}{L}\right),\\&\epsilon_{b+w}=\left(\frac{4\pi^2}{\beta L}\right)\left(1+\frac{1}{\psi}\right)\frac{1}{\sinh 2kh+2kh}.\end{aligned}\right\} \quad \cdots\cdots(43)$$

From the comparison between the above equation and Eq. (40), the relationship between ϵ_b and ϵ_{b+w} can be expressed as

$$\epsilon_b=\left\{\frac{\psi}{(1+\psi)}\right\}\epsilon_{b+w} \quad \cdots\cdots(44)$$

so that if ϵ_{b+w} is found by the experiment the wave decay modulus ϵ_b due only to bottom friction without the effect of the side walls can be calculated by Eq. (44). Referring to Eq. (37), the effect of the convective terms on ϵ_b is expected to be fairly large when the energy dissipation due to side wall friction is taken into account.

Regarding the wave damping due to water surface friction, Van Dorn[25] derived the surface damping coefficient by calculating the energy dissipation due to the viscosity of water in the boundary layer developing on the water surface under the assumption that the surface is horizontally immobilized.

According to his idea, the wave decay modulus ϵ_s for the energy dissipation on the water surface is expressed as follows:

$$\epsilon_s=\left(\frac{4\pi^2}{\beta L}\right)\frac{\cosh^2 kh}{\sinh 2kh+2kh}. \quad \cdots\cdots(45)$$

Denoting the average energy dissipation on the water surface by $\bar{E}_{fs}$, the ratio of $\bar{E}_{fs}$ to the bottom energy dissipation $\bar{E}_{fb}$ becomes

$$\frac{\bar{E}_{fs}}{\bar{E}_{fb}}=\cosh^2 kh. \quad \cdots\cdots(46)$$

Consequently the estimation by Van Dorn's method leads to the conclusion that the wave energy dissipation on the water surface is always more than that on the bottom, which is surely questionable in the normal sense.

Now, neglecting the vertical motion of oscillatory waves and assuming that the boundary layer does not develop in water but in air, the average energy dissipated in the boundary layer of air can be expressed as follows in reference to that on the bottom:

$$\bar{E}_{fs}=\frac{\mu_a}{2}\left(\frac{\pi}{\nu_a T}\right)\left(\frac{\pi H}{T}\right)^2\frac{\cosh^2 kh}{\sinh^2 kh}. \quad \cdots\cdots(47)$$

Therefore, the ratio of $\bar{E}_{fs}$ to that on the bottom becomes

$$\frac{\bar{E}_{fs}}{\bar{E}_{fb}}=\frac{\mu_a\sqrt{\nu}}{\sqrt{\nu_a}\mu}\cosh^2 kh, \quad \cdots\cdots(48)$$

in which μ_a and ν_a are the dynamic and kinematic viscosities of air respectively.

Computing Eq. (48) using adequate values of ν, ν_a μ, and μ_a, it is found that the average energy dissipation on the water surface is, at most, as little as 1% of the bottom dissipation. Therefore, the influence of surface dissipation on the wave damping may be neglected.

(c) *Relationships between bottom friction factor, bottom friction coefficient and wave decay modulus* In the study of wave damping by wave observations, the

estimation of the bottom friction factor has been usually made by using the following relationship for the bottom shearing stress, defined by Bretschneider[30]:

$$\tau_b=\rho f u_b^2, \quad \cdots\cdots(49)$$

in which f is the so-called bottom friction factor, and u_b the velocity component of water particles on the bottom, which is equivalent to U presented before. The rate of wave energy dissipation $\bar{E}_{fb}'$ derived by the definition of Eq. (49) can be written as

$$\bar{E}_{fb}'=\left(\frac{4}{3\pi}\right)\rho f u_0^3. \quad \cdots\cdots(50)$$

Then assuming that the rate of energy dissipation based on the linearized theory equalizes Eq. (50), the following expression is obtained for the bottom friction factor:

$$f=\left(\frac{3\pi\sqrt{\pi}}{8}\right)R_{eT}^{-\frac{1}{2}}. \quad \cdots\cdots(51)$$

Consequently, from the comparison between Eqs. (22) and (51), the relation between f and $\bar{C}_f$ can be expressed as

$$f=\left(\frac{3\pi^2}{64\sqrt{2}}\right)\bar{C}_f, \quad \cdots\cdots(52)$$

and from Eqs. (41) and (51) the relationship between ϵ_b and f can be written as

$$f=\left(\frac{3}{32\pi}\right)\epsilon_b\left(\frac{H}{L}\right)^{-1}\left\{\sinh kh(\sinh 2kh+2kh)\right\}. \quad \cdots\cdots(53)$$

In addition, the formula of wave damping based on Eq. (50) is expressed by

$$\frac{H}{H_0}=1-\left(\frac{8}{3\pi\sqrt{\pi}}\right)f\epsilon_b R_{eT}^{\frac{1}{2}}\left(\frac{x}{L}\right). \quad \cdots\cdots(54)$$

3. Experiments on bottom shearing stress and wave damping

(1) Measurement of bottom shearing stress

There are two methods for determining experimentally the bottom shearing stress in the case of a laminar boundary layer. One is to find the value of τ_b indirectly from the measurement of the velocity distribution, and the other is by the direct measurement of the shearing stress on a bottom surface. The latter was employed in the present study and a measuring device similar to that used by Eagleson (1959) was made.

(a) *Characteristics of the measuring device* Fig. 3 shows a schematic view of the measuring device. It consists of three main parts, which are a moment meter, a supporting rod and a flat plate. First of all, basic investigations of the characteristics of the device were carried out. Although the details are omitted here, this investigation yielded the following results: (1) It is desirable to reduce the masses of the shear plate and the supporting rod as much as possible. (2) If

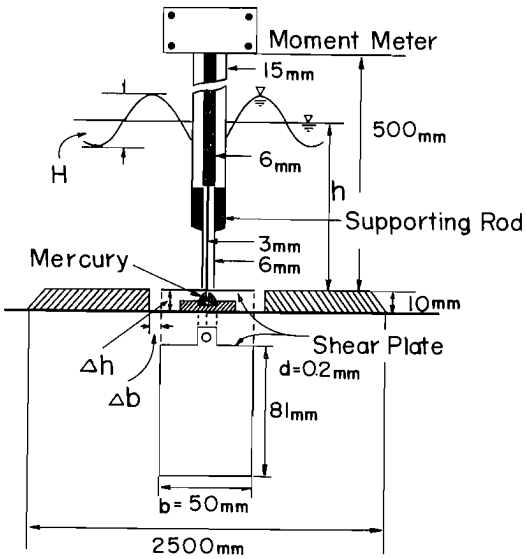

Fig. 3. Schematic diagram of shear meter.

the shear plate slips upward from the bottom, the shearing stress is overestimated owing to the drag force acting on the edges of the shear plate; conversely, if the shear plate slips downward, there is no appreciable effect. (3) The larger the clearance Δh under the shear plate, the smaller the experimental value of the shearing stress becomes, and the more the value tends to approach the theoretical one. (4) The less the clearance gap between the shear plate and the bottom surface Δb, the smaller the experimental value becomes, and the more the value tends to approach the theoretical one. (5) The thinner the shear plate, the smaller the experimental value becomes, and the more the value tends to approach the theoretical one. (6) If the shear plate is made smaller and the supporting rod is made lighter, the experimental value becomes small and approaches the theoretical one. (7) The width of the shear plate b has little effect, but the influence of the shield pipe on the shearing stress will appear if the width is too small.

On the basis of these results, a shear plate which is 8.1 cm long, 5 cm wide, 0.2 mm thick and made of stainless steel was finally chosen to be used. Furthermore, to prevent flow through the clearance under the plate, a small channel, 3 mm wide, running from wall to wall of the recess in the transverse direction, similar to that used by Eagleson, was made and filled with mercury until the meniscus touched the underside of the plate. In addition, the supporting rod was connected with the shear plate at the edge of the plate, and both the supporting rod and the shield pipe were made finer at the lower end, as shown in Fig. 3, so as to remove the influence of the shield pipe on the shearing stress measurement as much as possible.

(b) *Experimental procedures* The characteristics of waves and water depths used in the experiment are shown in Table 1, in which (1) indicates the experiment made in 1964 by using a plunger-type wave generator and (2) shows what was

made in 1965 by using a flutter-type one. The shearing stress acting on the bottom was measured for various wave characteristics. Wave heights were recorded by electric resistance type wave meters in a pen-writing oscillograph.

Table 1 Characteristics of waves and water depths used in the measurement of bottom shearing stress.

(1) Experiment made in 1964

Water depth h(cm)	Wave period T(sec)	Wave height H(cm)
8.2～29.3	0.85	0.63～3.64
9.0～34.3	0.95	0.48～3.64
9.0～29.0	1.10	0.77～3.75
11.0～34.1	1.30	0.65～3.03

(2) Experiment made in 1965

Water depth h(cm)	Wave period T(sec)	Wave height H(cm)
7.0	0.99～1.50	0.26～0.31
10.0	0.99～1.49	0.21～0.95
15.0	0.95～2.5	0.39～3.49
20.0	0.88～3.0	0.61～6.45
25.0	1.01～2.0	4.67～6.84
30.0	1.01～2.58	0.81～10.0

(c) *Results of experiment and considerations* In order to estimate exactly the shearing stress from the measurement of the force acting on the shear plate, a correction for the forces acting on the plate other than the shearing force is necessary. The external force F is assumed to be equal to the sum of three forces: the shearing force, the force resulting from pressure gradients acting on both sides of the plate and the virtual mass force. Since, however, flow under the shear plate is prevented by injecting mercury into the small channel, it is doubtful whether the virtual mass force acts on the plate; therefore, the virtual mass force is neglected in this case, and the experimental values are examined on the basis of the linearized theory, assuming that the effect of the convective terms presented before is omitted.

Denoting the surface area of the shear plate by A, and the thickness by d, the shearing force acting on the plate can be written from Eq. (18) as

$$\tau_0 A=\mu\frac{Akc\beta H}{2\sinh kh}\{\sin(\xi-\tau)-\cos(\xi-\tau)\} \quad \cdots\cdots(55)$$

and the force resulting from pressure gradients can be expressed as

$$-Ad\frac{\partial p}{\partial x}=-\frac{\rho gkHAd}{2\cosh kh}\cos(\xi-\tau)\,, \quad \cdots\cdots(56)$$

so that the horizontal force F per unit area acting on the shear plate is written as

$$F=\frac{F'}{A}=-\sqrt{C^2+(C+D)^2}H\sin(\xi-\tau+\varepsilon') \quad \cdots\cdots(57)$$

in which

$$\left.\begin{aligned} &C=\frac{\mu kc\beta}{2\sinh kh}\,, \quad D=\frac{\rho gkd}{2\cosh kh}\,, \\ &\varepsilon'=\tan^{-1}\left(1+\frac{D}{C}\right), \quad \frac{D}{C}=2\beta d. \end{aligned}\right\} \quad \cdots\cdots(58)$$

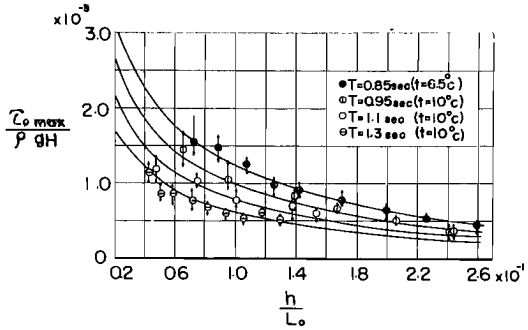

Fig. 4. Comparisons between theoretical curves and experimental results of maximum bottom shearing stress with correction.

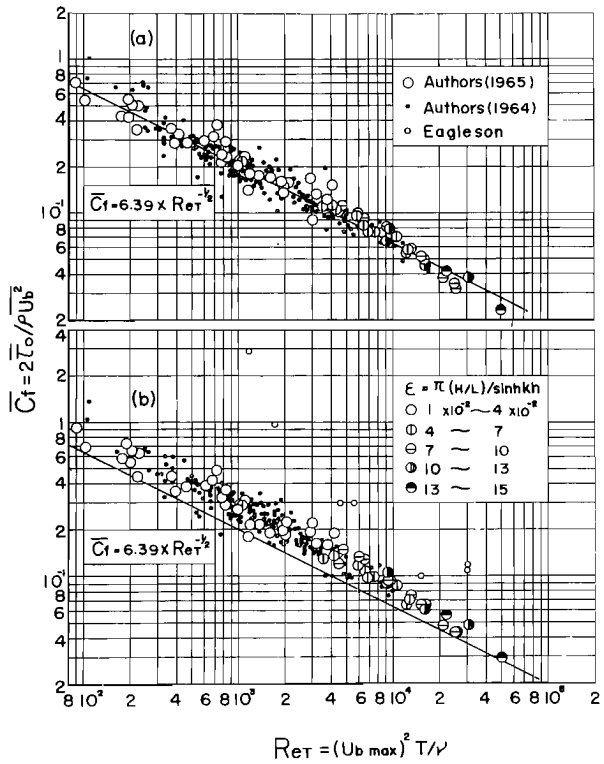

Fig. 5. Relation between average friction coefficient $\bar{C}_f$ and Reynolds number R_{eT}.
(a) With correction of pressure force
(b) Without correction of pressure force

Therefore, the relationship between the maximum measured horizontal force per unit area F_{max} and the maximum shearing stress $\tau_{0\,max}$ can be expressed from Eqs. (55) and (57) as

$$\tau_{0\,max}=\left\{\frac{2}{1+(1+2\beta d)^2}\right\}^{\frac{1}{2}}F_{max}. \quad \cdots\cdots(59)$$

Fig. 4 shows the relation between $\tau_{0\,max}/\rho gH$ and h/L_0 with a parameter of the wave period, in which L_0 is the deep water wave length. The experimental data were corrected by applying Eq. (59). In this figure, arrows at each experimental value indicate the range of scatter, and circular points are the corresponding mean values. It may be seen from the figure that experimental results agree well with the theoretical values computed from the linearized theory.

The comparison between the theoretical bottom friction coefficients and the experimental values obtained from the direct measurement of shearing stresses is shown in Fig. 5 against the wave Reynolds number of R_{eT}. The experimental values shown in (a) of this figure are the data obtained by correcting on the basis of Eq. (59) for the horizontal force due to pressure gradient, and the values shown in (b) are the uncorrected data. Eagleson's data are also shown in the same figures. They are very much larger than the authors' results and considerably scattered. A possible reason for this is that the shear plates used by Eagleson were much larger than those used by the authors, so that the forces other than the shearing force predominatingly acted on the shear plate, and that therefore the correction method for these forces was inadequate. It may be seen from these figures that the experimental values corrected $\overline{C}_f$ agree well with the theoretical ones, but the uncorrected values are 30% to 40% larger than the theoretical ones. This is the result to be expected from the theoretical consideration of the effect of the convective terms, and it is concluded that the effect can be neglected within

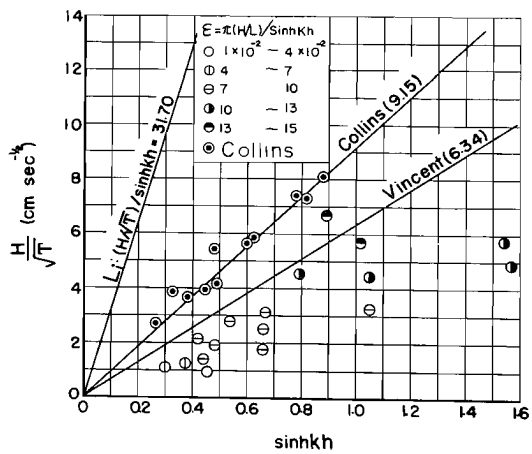

Fig. 6. Examination of experimental result by Collins' criterion for transition from laminar to turbulent boundary layer.

the range of the present experiments. In addition, some of the authors' experimental values examined by the criterion of Collins[31] for the transition from laminar to turbulent boundary layer are shown in Fig. 6, in which the values of $(HT^{-1/2})$ are plotted against sinh kh and the legends correspond to those in Fig. 5. The criteria of *Li*[32] and Vincent[33] on the basis of the experimental values are also shown in the figure. Since the value of R_{eT} corresponding to Collins' criterion becomes 8.03×10^4 in this case, it can be seen from the figure and Fig. 5 that the authors' data are all in the region of the laminar boundary layer. Since the maximum value of R_{eT} in the experimental data is about 5×10^4, it is necessary to perform further experiments in a wider region involving higher values of R_{eT} to clarify the wave damping characteristics in the transition from laminar to turbulent boundary layer.

(2) Experiment on wave damping

(a) *Experimental equipment and procedures* The wave channel, the wave generators and the wave meters used in the experiments were the same as those used in the experiment on shearing stresses. Characteristics of waves and water depths in the experiment are presented in Table 2, in which (1) and (2) indicate the experiments performed in 1964 and 1965 respectively. As shown in Fig. 7, stations for the measurement of wave height were S-1, 15 m from the flutter-type

Table 2 Characteristics of waves and water depths used in the experiment on wave damping.

(1) Experiment made in 1964

Water depth h(cm)	Wave period T(sec)	Wave height H(cm)
10.8~24.6	0.80	1.66~6.00
12.0~28.5	1.00	1.53~7.03
25.9	1.10	4.50~6.85
16.3~30.0	1.30	2.40~6.05

(2) Experiment made in 1965

Water depth h(cm)	Wave period T(sec)	Wave height H(cm)
5.6	0.80	0.099~0.117
9.9	0.99~1.23	2.22 ~2.89
10.0	1.00~1.47	0.27 ~1.31
11.0	0.80	1.74
13.6	0.85~1.53	0.969~1.82
15.0	0.94~1.85	0.442~3.98
16.5	1.01~1.53	1.33 ~2.28
17.0	0.80	4.04
20.0	0.87~2.09	0.497~7.38
20.6	1.15~2.02	1.69 ~3.69
23.1	1.02~2.00	2.15 ~4.50
25.0	0.97~2.01	3.55 ~7.55
30.0	1.00~2.00	1.35 ~11.2
35.0	1.15~2.02	0.410~4.10
40.0	1.23~1.54	1.71 ~6.67
45.0	1.30~2.28	2.35 ~3.62

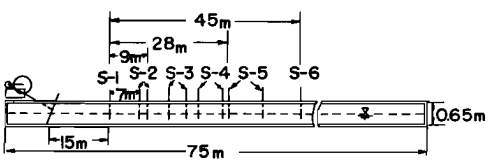

Fig. 7. Stations of wave meters.

wave generator, and S-2, S-3, S-4, S-5 and S-6 at intervals of 9 m or 7 m in the case of the experiment (2), and were S-1, 9 m from the plunger-type wave generator and the other four stations at intervals of 7.2 m from each other in the case of the experiment (1).

Wave heights at the five or six stations were recorded at the same time. Owing to the limitations of the instrument, part of them were measured successively at each station, the wave period being kept constant, and then determined by taking an average of five to ten wave heights when the wave train was uniform, or twenty wave heights when the wave train was somewhat scattered.

(b) *Results of the experiment* The measurements were made by changing the water depth or the length of the stroke of the generator for each wave period as presented in Table 2, and plotting the experimental values of wave height on semi-log scale paper; the wave height decreased linearly with the distance x as seen in Fig. 8 and the following relationship already derived theoretically in Eq. (43) could be verified:

$$\frac{H}{H_0}=\exp\{-\alpha_{b+w}x\}, \quad \cdots\cdots(60)$$

in which α_{b+w} is the damping coefficient including the influences of the bottom and side walls of the wave channel.

From Eqs. (40), (43) and (60), the relationships between α_{b+w} and ϵ_{b+w}, α_b and ϵ_b are expressed respectively as

$$\alpha_{b+w}L=\epsilon_{b+w},\ \alpha_bL=\epsilon_b. \quad \cdots\cdots(61)$$

Therefore, by drawing a fitted straight line in the figure, the wave decay modulus can be calculated from Eq. (61). As the value of ϵ_{b+w} varies widely

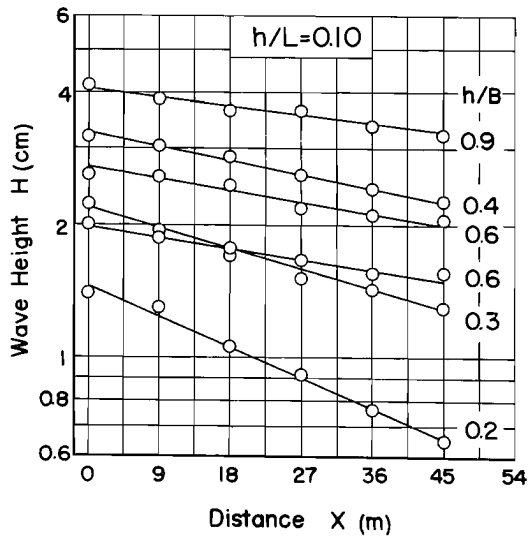

(1)

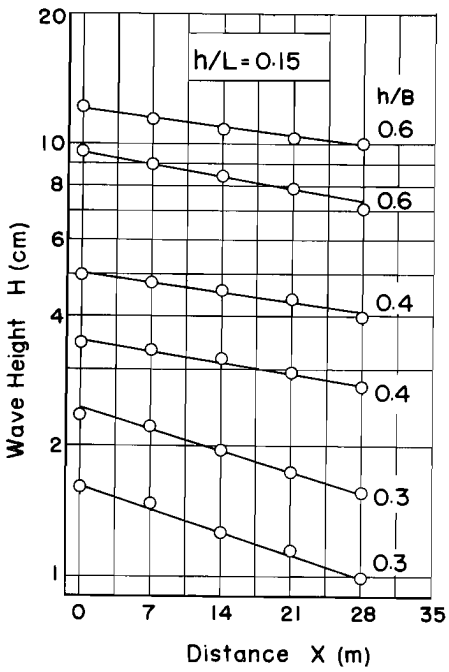

(2)

Fig. 8. Some examples of experimental results of wave height attenuation with distance.

according to the manner of drawing a straight line, however, the following method was used. For practical purposes, the value of ϵ_{b+w} must be obtained from the wave heights at two stations, H_0 and H_1 and the distance x between them. Wave heights at several pairs of stations were accordingly used for the purpose of taking the average. Thus, the damping coefficients were calculated by Eqs. (60) and (61) and then the values of ϵ_b were obtained by applying Eq. (44).

Next, the comparison between the experimental results and the theoretical formula of wave damping already mentioned will be discussed. Transforming Eq. (43) by using the result of the linearized theory, the following relationship can be obtained:

$$\beta L\epsilon_{b+w}=1+\left(\frac{1}{\psi_0}\right)\frac{4\pi^2}{\sinh 2kh+2kh}, \quad \cdots\cdots(62)$$

in which $\psi_0=kB/\sinh 2kh$. Hence it is possible to examine the influences of relative depth, h/L, and the ratio of the water depth to the width of the water tank, h/B, on the wave decay modulus.

Fig. 9 shows an example of the experimental results, in which the influence of h/L on the values of $\beta L\epsilon_{b+w}$ is examined by keeping the value of h/B constant. The curve in the figure indicates the theoretical relation. From the experimental results made for several values of h/B, it was found that, although the experi-

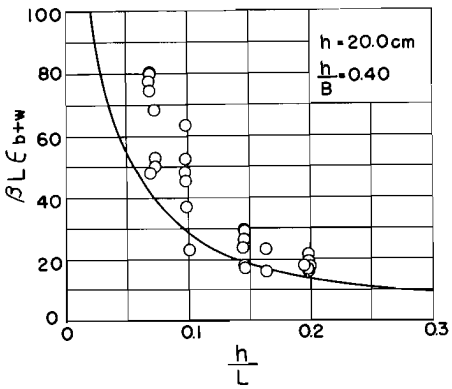

Fig. 9. Effect of relative depth h/L on wave decay modulus.

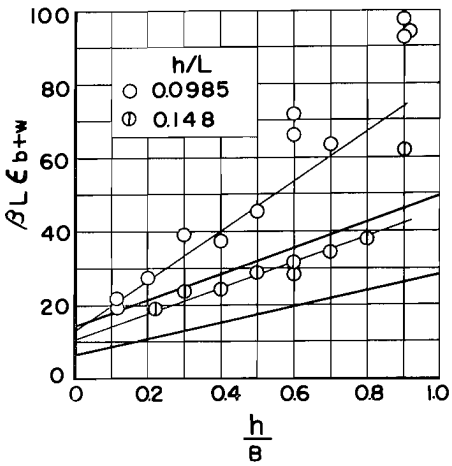

Fig. 10. Example of effects of side walls on wave decay modulus.

mental values are widely scattered, the tendency of the plotted data is closely similar to that of the theoretical curve. But the experimental values are, as a whole, larger than the theoretical ones.

According to the small amplitude wave theory, wave steepness has no influence on wave damping. In order to make sure of this fact some experiments were carried out by changing the wave height only, the water depth and wave period being kept constant. The experiments showed that there is no influnce of wave steepness on the wave decay modulus for any value of h/L.

Keeping the value of h/L constant and plotting the relation between $\beta L\epsilon_{b+w}$ and h/B, the effect of the side walls on the wave damping can be examined. Fig. 10 shows an example of the experimental results, where the experimental values are seen as a whole to be fairly large in comparison with the theoretical curves expressed by thick solid lines. The tendency seems to be remarkable, when the value of h/L is small and the value of h/B is large.

Fig. 11 shows the comparison between the experimental values of the wave decay modulus and theoretical ones for the two cases ; one is based on the linearized theory and the other on the non-linear theory in which the effect of the convective terms is taken into account. (a) indicates the former and (b) the latter. In this case, the data were used after taking an average of each experimental result for the same water depth and wave period. In this figure, the experimental results obtained by Watson and Martin, Grosch and Lukasik, and Eagleson are plotted in addition to the authors' results. It is found from the comparison that the experimental values of ϵ_b are nearly as much as 40% larger than the theoretical ones based on the linearized theory, but when corrected theoretically for the side wall effect based on the non-linear theory, the experimental values decrease by as much as 10% and approach more closely to the theoretical ones. The data of Grosch and Lukasik were obtained from the experiment on wave damping in a wide wave channel whose width can be neglected as far as the side wall effect is

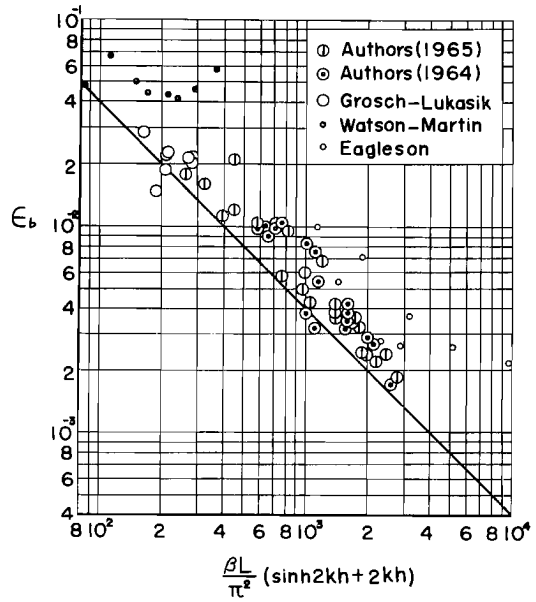

(a) By linear theory

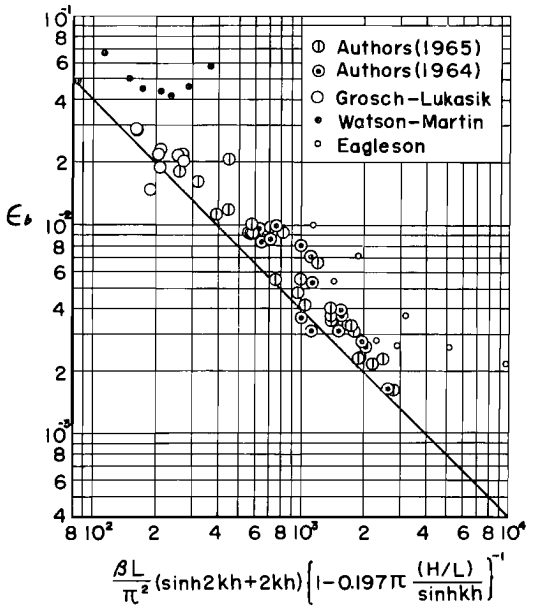

(b) By non-linear theory

Fig. 11. Comparisons between theoretical relationships and experimental results of dimensionless decay modulus.

concerned, while Eagleson's data are values calculated from the results of the direct measurement of bottom shearing stresses. As mentioned previously, it may be seen that Eagleson's data give much larger values for ϵ_b than those obtained by the authors and by Grosch and Lukasik.

From the above results, it is found that the effect of the convective terms on wave damping is approximately as much as 10% and yet the experimental values are as much as 30% larger than the theoretical ones. On the other hand, since the experimental values of $\beta L\epsilon_{b+w}$ shown in Fig. 10 change linearly, on the whole, with the value of h/B, if a fitted straight line drawn through the experimental values holds true in the region near $h/B=0$, the value of $\beta L\epsilon_b$ can be determined as the value of $\beta L\epsilon_{b+w}$ at $h/B=0$. Therefore, this value can be regarded as that without the side wall effect. The results obtained in this manner are compared with the relationship of the linearized theory in Fig. 12. Even from these results, however, it is found that the experimental values found by the authors and by Grosch and Lukasik are still approximately 20% larger than the theoretical ones.

In addition, the value of the bottom friction factor f calculated from the experimental results on wave damping by means of Bretschneider's method will be described briefly. The following relationship of wave energy conservation is used in this case:

$$B(C_g E_1 - C_g E_2) = l\{\bar{E}_{fb}' B + 2\bar{E}_{fw} h\}, \quad \cdots\cdots(63)$$

in which E_1 and E_2 are the average wave energies per unit surface area over one

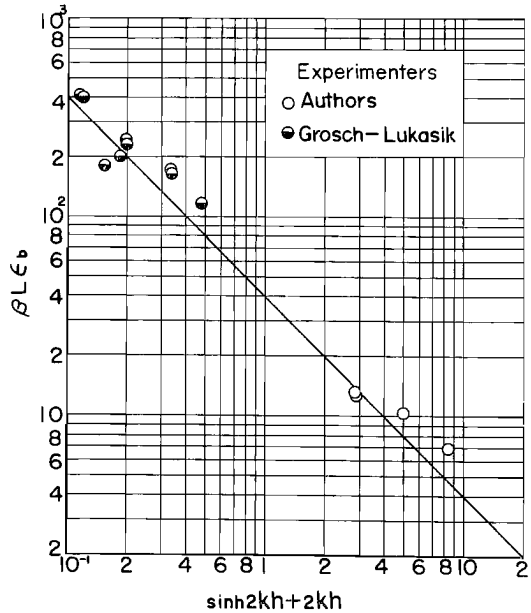

Fig. 12. Comparison between theoretical relation and experimental results of $\beta L\epsilon_b$ obtained by extrapotation.

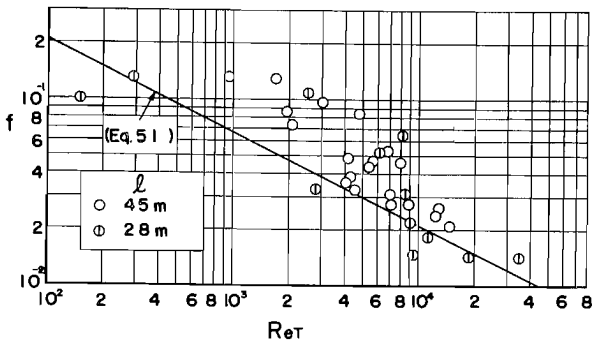

Fig. 13. Relation between bottom friction factor f and wave Reynolds number R_{eT}.

wave period at the two selected wave meters, l is the distance between them, and $\bar{E}_{fb}'$ and $\bar{E}_{fw}$ refer to Eq. (50) and (37) respectively.

Fig. 13 shows the comparison between the values of f calculated from Eq. (63) and the theoretical result on the basis of Eq. (51). It is found from the figure that the experimental values are as a whole larger than the theoretical ones as presented in Figs. (11) and (12).

In the above description, although the reasons why the experimental values of wave damping appear larger than the theoretical ones are not yet perfectly clear, the following suggestions may be put forward: One of the reasons may lie in the application of the wave theory to the theory of wave damping, though Airy's wave theory was applied in the present paper, and it is necessary to analyze the damping characteristics of finite amplitude waves, such as Stokes' waves. Secondly, there may be a problem of the transition from laminar to turbulent boundary layers resulting from oscillatory wave motion. Although all of the authors' data described above were in the laminar region according to the criterion of Collins[31] for the transition, there are wide differences between the criteria of different authorities. This problem must be investigated in detail on the basis of further experimental work. Thirdly, the wave energy dissipation on the water surface resulting from wave motion must be taken into account, and two factors may be considered for this reason: One is the effect of surface tension, which was examined experimentally by Keulegan[34] for the damping of standing waves and the other the relative motion between air and water as mentioned previously. The authors wish to investigate such problems through further detailed experiments and to discover the mechanism of wave damping due to bottom friction.

4. Conclusion

As described above, the authors established a theory of the laminar damping of oscillatory waves based on an approximate solution of the laminar boundary layer equation, and measured the bottom shearing stress and the decay modulus of oscillatory waves. It is concluded that the influences of the convective terms in the basic equation on the bottom shearing stress and the wave energy dissipa-

tion in the boundary layer on the bottom are negligible within the range of the experiments, but those on the side walls of a wave channel are considerable, that is about 20% at maximum within the range of the authors' experiment; accordingly the experimental values of the shearing stresses on the bottom agree well with the result of the linearized theory if the data are corrected for the pressure force. With regard to wave damping it was concluded that the experimental values of the wave decay modulus are approximately 40% larger than those derived from the linearized theory and even if they are corrected for the effect of the convective terms, they are still approximately 30% larger than the theoretical ones. It would seem that the discrepancy is due to the existence of some other energy dissipations.

5. Acknowledgement

Part of this investigation was accomplished with the support of the Science Research Fund of the Ministry of Education, for which the authors express their appreciation. Thanks are due to Mr. J. Takashina, a former student of Kyoto Univ., for his help during this investigation and Mr. T. Shibano, Misses S. Ichiju and S. Sakata for their help in preparing the paper.

References

1) Lamb, H: Hydrodynamics, 6th Edition, New York, Dover Publications, 1945, pp. 619~623.
2) Hough, S. S.. On the Influence of Viscosity on Waves and Currents, Proc. London Mathematical Society, Vol. 28, 1896, pp. 264~288.
3) Biesel, F.: Calcul de L'amortissement d'une Houle dans un Liquide Visqueux de Profondeur Finie, La Houille Blanche, 1949, pp. 630~634.
4) Putnam, J. A. and Johnson, J. W.. The Dissipation of Wave Energy by Bottom Friction, Trans. AGU, Vol. 30, 1949, pp. 67~74.
5) Savage, R. P.: Laboratory Study of Wave Energy by Bottom Friction and Percolation, BEB, Tech. Memo. No. 31, 1953, pp. 1~25.
6) Putnam, J. A.: The Dissipation of Wave Energy by Flow in a Permeable Sea Bottom, Trans. AGU, Vol. 30, 1949, pp. 349~356.
7) Reid, R. O. and Kajiura, K.: On the Damping of Gravity Waves Over a Permeable Sea Bed, Trans. AGU, Vol. 38, No. 5, 1957, pp. 662~666.
8) Hunt, J. N.: On the Damping of Gravity Waves Propagated over a Permeable Surface, J. Geophs. Res., Vol. 64, No. 4, 1959, pp. 437~442.
9) Murray, J. D.: Viscous Damping of Gravity Waves over a Permeable Bed, J. Geophs. Res., Vol. 70, No. 10, 1965, pp. 2325~2331.
10) Kishi, T.: Studies on Sea Dikes (5)—Energy Dissipation of Shallow Water Waves Due to Bottom Friction—, Report, Pub. Works Res. Inst., No. 93, 1954, pp. 1~9 (in Japanese).
11) Iwagaki, Y. and Kakinuma, T.: On the Bottom Friction Factor of Akita Coast, Coastal Eng. in Japan, Vol. 6, 1963, pp. 83~91.
12) Iwagaki, Y. and Kakinuma, T.: On the Transformation of Ocean Wave Spectra in Shallow Water and the Estimation of the Bottom Friction Factor, Annuals, D. P. R. I., Kyoto Univ., No. 8, 1965, pp. 379~396 (in Japanese).
13) Eagleson, P. S.: The Damping of Oscillatory Waves by Laminar Boundary Layers, MIT, Hydrodynamics Laboratory, Tech. Rep. No. 32, 1959, pp. 1~37.
14) Eagleson, P. S.: Laminar Damping of Oscillatory Waves, Proc. ASCE, Vol. 88, No. HY 3, 1962, pp. 155~181.
15) Grosch, C. E., Ward, L. W. and Lukasik, S. J.: Viscous Dissipation of Shallow Water

Waves, Physics of Fluids, Vol. 3, No. 3, 1960, pp. 477～479.
16) Grosch, C. E. and Lukasik, S. J.: Discussion of "Laminar Damping of Oscillatory Waves", Proc. of ASCE, Vol. 89, No. HY1, 1963, pp. 232～293.
17) Tsuchiya, Y. and Inoue, M.. Basic Studies on the Wave Damping Due to Bottom Friction (First Report), Proc. of 8th Conf. of Coastal Eng. in Japan, 1961, pp. 19～24 (in Japanese).
18) Iwagaki, Y., Tsuchiya, Y. and Sakai, M.: Basic Studies on the Wave Damping Due to Bottom Friction (Second Report)—On the Measurement of Bottom Shearing Stresses—, Proc. of 11th Conf. of Coastal Eng. in Japan, 1964, pp. 62～68 (in Japanese).
19) Iwagaki, Y., Tsuchiya, Y. and Chen, H.: Basic Studies on the Wave Damping Due to Bottom Friction (Third Report)—On the Influence of Convective Terms in the Laminar Boundary Layer Equations—, Proc. of 12th Conf. of Coastal Eng. in Japan, 1965, pp. 41～49 (in Japanese).
20) Iwagaki, Y., Tsuchiya, Y. and Sakai, M.: Basic Studies on the Wave Damping Due to Bottom Friction, Coastal Engineering in Japan, Vol. 8, Dec. 1965, pp. 37～49.
21) Kajiura, K.: On the Botton Friction in an Oscillatory Current, Bulletin of the Earthquake Research Institute, Vol. 42, 1964, pp. 147～174.
22) Jonsson, I. G.: Wave Boundary Layers and Friction Factors, Proc. 10th Conf. on Coastal Engineering, 1966 (printing).
23) Jonsson, I. G.: Friction factor Diagrams for Oscillatory Boundary Layers, Basic Research-Progress Report, Coastal Eng. Lab., Tech. Univ. of Denmark, No. 10, Dec. 1965, pp. 10～21.
24) Jonsson, I. G.. Measurements in the Turbulent Wave Boundary Layer, I. A. H. R., 10th Congress, London, Vol. 1, 1963, pp. 85～92.
25) Van Dorn, W. G.: Boundary Dissipation of Oscillatory Waves, J. of Fluid Mech., Vol. 24, Part 4, 1966, pp. 769～779.
26) Iwasa, Y.: Attenuation of Solitary Waves on a Smooth Bed, Trans. ASCE, Vol. 124, 1959, pp. 193～206.
27) Grosch, C. E.. Laminer Boundary Layer under a Wave, Physics of Fluids, Vol. 5, No. 10, 1962, pp. 1163～1167.
28) Schlichting, H.: Boundary Layer Theory, McGraw Hill, New York, 1960, p. 207.
29) Longuet-Higgins, M. S.: Supplement to a Paper by R. C. H. Russell and J. P. C. Osorio, Proc. 6th Conf. Coastal Eng., Univ. of Florida, 1957, pp. 184～193.
30) Bretschneider, C. L.. Field Investigation of Wave Energy Loss of Shallow Water Ocean Waves, BEB, Tech. Memo., No. 46, 1959, pp. 1～21.
31) Collins, J. I.. Inception of Turbulence at the Bed under Periodic Gravity Waves, J. of Geophs. Res., Vol. 68, 1963, pp. 6007～6014.
32) Li, H.: Stability of Oscillatory Laminar Flow near an Oscillating Wall, BEB, Tech. Memo., No. 47, 1954, pp. 1～48.
33) Vincent, G. E.. Contribution to the Study of Sediment Transport on a Horizontal Bed Due to Wave Action, Proc. 9th Conf. Coastal Eng., Univ. of Florida, 1958, pp. 326～354.
34) Keulegan, G. H.: Energy Dissipation in Standing Waves in Rectangular Basin, J. of Fluid Mech., No. 6, 1958, pp. 33～50.